The Plant Cell, Vol. 30: 196–208, January 2018, www.plantcell.org © 2018 ASPB.

The Plastid Lipocalin LCNP Is Required for Sustained Photoprotective Energy Dissipation in Arabidopsis[OPEN]

Alizée Malnoë,[a,1] Alex Schultink,[b] Sanya Shahrasbi,[b] Dominique Rumeau,[c] Michel Havaux,[c] and Krishna K. Niyogi[a,b,d,1]

[a] Molecular Biophysics and Integrated Bioimaging Division, Lawrence Berkeley National Laboratory, Berkeley, California 94720
[b] Department of Plant and Microbial Biology, University of California, Berkeley, California 94720
[c] CEA, CNRS UMR 7265, Biologie Végétale et Microbiologie Environnementales, Aix-Marseille Université, Laboratoire d'Ecophysiologie Moléculaire des Plantes, Saint-Paul-lez-Durance 13108, France
[d] Howard Hughes Medical Institute, University of California, Berkeley, California 94720

ORCID IDs: 0000-0002-8777-3174 (A.M.); 0000-0002-7936-782X (A.S.); 0000-0003-1110-0325 (S.S.); 0000-0001-7052-0448 (D.R.); 0000-0002-6434-393X (M.H.); 0000-0001-7229-2071 (K.K.N.)

Light utilization is finely tuned in photosynthetic organisms to prevent cellular damage. The dissipation of excess absorbed light energy, a process termed nonphotochemical quenching (NPQ), plays an important role in photoprotection. Little is known about the sustained or slowly reversible form(s) of NPQ and whether they are photoprotective, in part due to the lack of mutants. The *Arabidopsis thaliana suppressor of quenching1* (*soq1*) mutant exhibits enhanced sustained NPQ, which we term qH. To identify molecular players involved in qH, we screened for suppressors of *soq1* and isolated mutants affecting either chlorophyllide *a* oxygenase or the chloroplastic lipocalin, now renamed plastid lipocalin (LCNP). Analysis of the mutants confirmed that qH is localized to the peripheral antenna (LHCII) of photosystem II and demonstrated that LCNP is required for qH, either directly (by forming NPQ sites) or indirectly (by modifying the LHCII membrane environment). qH operates under stress conditions such as cold and high light and is photoprotective, as it reduces lipid peroxidation levels. We propose that, under stress conditions, LCNP protects the thylakoid membrane by enabling sustained NPQ in LHCII, thereby preventing singlet oxygen stress.

INTRODUCTION

Photosynthesis is a biological process of primary importance, as it provides the energy that drives food, feedstock, and biofuel production and mitigates climate change. Light in excess of photosynthetic capacity can lead to cellular damage (Li et al., 2009b). Thus, various ways to protect against photodamage have evolved, including ways to minimize light absorption, detoxify reactive oxygen species generated by excess light, and dissipate excess absorbed light energy (Horton et al., 1996). Together, these processes are known as photoprotection. The harmless dissipation of excess absorbed light energy as heat is commonly called nonphotochemical quenching (NPQ). The term NPQ originated from the way this process is assayed through monitoring a decrease (or quenching) of chlorophyll fluorescence. In contrast, photochemical quenching of chlorophyll fluorescence reflects photochemistry, the process in which light energy is converted to chemical energy in the form of ATP and NADPH. Despite the physiological importance of photoprotection, the molecular mechanisms of NPQ that protect against sustained light stress remain largely unknown.

NPQ mechanisms have been classified according to their relaxation kinetics and their sensitivities to chemical inhibitors and mutations (Walters and Horton, 1993; Nilkens et al., 2010). From faster to slower relaxing components, energy-dependent quenching (qE; Krause et al., 1982), zeaxanthin-dependent quenching (qZ; Dall'Osto et al., 2005; Nilkens et al., 2010), quenching due to chloroplast movement (qM; Cazzaniga et al., 2013), and photoinhibitory quenching (qI; Krause, 1988) have been shown to contribute to NPQ, whereas quenching due to state transitions (qT) is considered to be a minor contributor to NPQ in saturating light (Nilkens et al., 2010). The relative contribution of each of these components in protecting PSII from photodamage and their occurrence under different conditions is not fully understood (Lambrev et al., 2012; Ruban, 2016).

qE, also referred to as the flexible mode of energy dissipation, is the most well-studied NPQ component, and its key molecular players have been identified. In vascular plants, the protein PsbS senses acidification of the lumen upon light exposure and, together with the xanthophyll pigment zeaxanthin, is necessary to catalyze the formation of a quenching site (Demmig et al., 1987; Niyogi et al., 1997; Li et al., 2000; Johnson and Ruban, 2011; Sylak-Glassman et al., 2014). Previously, we asked the question whether NPQ could be rescued in the absence of either of these key players. From a suppressor screen using the *Arabidopsis thaliana npq1* mutant, which lacks zeaxanthin, we found that the xanthophyll pigment lutein can partially replace the function of zeaxanthin (Li et al., 2009a). Through a suppressor screen using the *npq4* mutant lacking PsbS, we uncovered a slowly reversible form of NPQ, thus pertaining to qI, which is negatively regulated by SUPPRESSOR OF QUENCHING1 (SOQ1) (Brooks et al., 2013). qI comprises processes that relax slowly, such as photoinhibition, which is defined as the light-induced decrease in the quantum yield of photosynthetic carbon fixation. qI can be due to photooxidative

[1] Address correspondence to alizee.malnoe@umu.se or niyogi@berkeley.edu.
The authors responsible for distribution of materials integral to the findings presented in this article in accordance with the policy described in the Instructions for Authors (www.plantcell.org) are: Alizée Malnoë (alizee.malnoe@umu.se) and Krishna K. Niyogi (niyogi@berkeley.edu).
[OPEN]Articles can be viewed without a subscription.
www.plantcell.org/cgi/doi/10.1105/tpc.17.00536

damage to the D1 protein of PSII (Edelman and Mattoo, 2008). However, not all of qI is due to PSII photodamage, as there are slowly relaxing fluorescence quenching processes that are independent of D1 damage (Demmig and Björkman, 1987) or D1 function (Chow et al., 1989). The Arabidopsis *soq1* mutant is a genetic entry point into studying qI unrelated to PSII photodamage.

The form of NPQ negatively regulated by SOQ1 is independent of known components required for other types of NPQ, such as PsbS, zeaxanthin, ΔpH formation, or the STN7 kinase (Brooks et al., 2013). We now term this component qH to distinguish this photoprotective, slowly reversible NPQ from qI; like its position in the alphabet, the photoprotective quenching "H" comes before quenching due to PSII photodamage (and possibly other yet to be discovered, slowly relaxing photoinhibitory NPQ processes) "I." Sustained ΔpH-independent NPQ has been described in evergreens (Demmig-Adams et al., 2014), and we are now uncovering the molecular players involved in qH, which is a good candidate for this photoprotection mode. SOQ1 is a chloroplast-localized membrane protein of 104 kD that contains multiple domains, including a HAD phosphatase on the stromal side of the thylakoid membrane, a transmembrane helix, and thioredoxin-like and β-propeller NHL domains on the lumenal side of the thylakoid membrane. The stromal domain is dispensable for SOQ1 to negatively regulate NPQ, whereas the lumenal domains are required (Brooks et al., 2013).

To elucidate the mechanism of the NPQ component qH and to identify possible targets of SOQ1, we performed a suppressor screen on the *soq1 npq4* mutant and searched for mutants that no longer exhibited this slowly reversible NPQ. We proposed that SOQ1 is involved in reducing lumenal or lumen-exposed target proteins to prevent formation of slowly reversible antenna quenching, either directly or via another protein (Brooks et al., 2013). We expect that suppressors (in the classical genetic definition) of the enhanced quenching observed in the *soq1 npq4* mutant background might be mutated in the site of quenching or in a putative downstream target of SOQ1. By definition, the NPQ phenotype of these suppressors (triple mutants) will return to the initial low NPQ phenotype, which is that of *npq4*. Two types of mutants emerged from the screen, including one type affecting the peripheral antenna of PSII and one type identifying the likely downstream target of SOQ1. These findings confirm that qH occurs in the antenna, specifically in the peripheral antenna of PSII, and demonstrate that the plastid lipocalin is required for this quenching mechanism to occur.

RESULTS

Chlorophyllide *a* Oxygenase Suppressors Identify the Requirement of Chlorophyll *b* for qH

To elucidate qH further, we conducted a suppressor screen using the Arabidopsis *soq1 npq4* mutant. We chose this double mutant as the starting genotype to minimize the identification of mutations affecting PsbS-dependent qE or ΔpH formation. We generated an EMS-mutagenized M2 population and screened it by video imaging of chlorophyll *a* fluorescence for the suppression of qH. Out of 22,000 mutant individuals screened, a class comprising two independent mutants, #26 and #42, showed a pale-green phenotype and displayed NPQ kinetics similar to that of *npq4* (Figure 1A). HPLC analysis of pigments showed that the visible pale green phenotype was due to a lack of chlorophyll *b* (Figure 1B). This pigmentation phenotype has previously been observed in mutants defective in the gene encoding chlorophyllide *a* oxygenase (CAO), which is required for chlorophyll *b* synthesis (Espineda et al., 1999). Sequencing the *CAO* gene in mutants #26 and #42 revealed single base pair (C-to-T) mutations, resulting in Thr375Ile and Gln89STOP, respectively. As three mutant *CAO* alleles have been previously described in Arabidopsis (Hirono and Redei, 1963; Espineda et al., 1999; Oster et al., 2000), we named these new alleles *chlorina1-4* and *chlorina1-5*, respectively. To independently recapitulate these findings, we crossed *soq1* with the *chlorina1-3* mutant, which is another null allele of *CAO*. The *soq1 chlorina1-3* double mutant did not show additional quenching compared with *chlorina1-3* (Figure 1C), confirming the requirement of chlorophyll *b* for qH.

A Class of Suppressors from the Genetic Screen That Does Not Show a Pigment Defect

Another class comprising two independent mutants, #205 and #252, displayed NPQ kinetics similar to that of *npq4* (Figure 2A, blue and green curves) and showed a "normal green" phenotype with wild-type pigment content (Figure 2B, Table 1). The F1 progenies of a cross between these two suppressor mutants (homozygous for *soq1* and *npq4* but heterozygous for each new mutation) showed a low level of NPQ similar to that of *npq4* (Figure 2A, gray curve), indicating that the two mutations belong in the same complementation group. We therefore proceeded to the genetic analysis of only one of these two mutants (#205). The mutation in #205 is semidominant, as shown by the intermediate NPQ phenotype of the F1 progenies from the cross *soq1 npq4* x #205 (Figure 2A, orange curve). The low NPQ phenotype segregated in a 1:2:1 pattern in the F2 generation from this cross, indicating that the phenotype is caused by mutation of a single nuclear gene.

Identification of the Mutated Gene in Normal Green Suppressors Using Whole-Genome Sequencing

Mapping by sequencing in Arabidopsis has recently been proven successful in several studies to determine the causative mutation of a specific phenotype (Schneeberger et al., 2009; Sorek et al., 2015). To this aim, we backcrossed the mutant #205 to the parental strain *soq1 npq4* used for the EMS mutagenesis and selected individuals that lacked qH from the F2 progeny (which represent one-quarter of the individuals with genotype *soq1 npq4* and homozygous for the new mutation). Genomic DNA was extracted from a pool of 75 F2 seedlings exhibiting the mutant phenotype and subjected to whole-genome sequencing. The sequencing reads were mapped onto the Col-0 Arabidopsis reference genome with ~100× average coverage (Supplemental Table 1), and single nucleotide polymorphisms were identified. The position and frequency of each single nucleotide polymorphism were plotted to look for a region of the genome showing enrichment in the allelic frequency of segregating mutations (Supplemental Figure 1). An increase in the allelic frequency of mutations approaching 100% was observed in the region between 16.5 and 21 Mb on chromosome 3, identifying this region as the one containing the causative mutation. We sequenced the

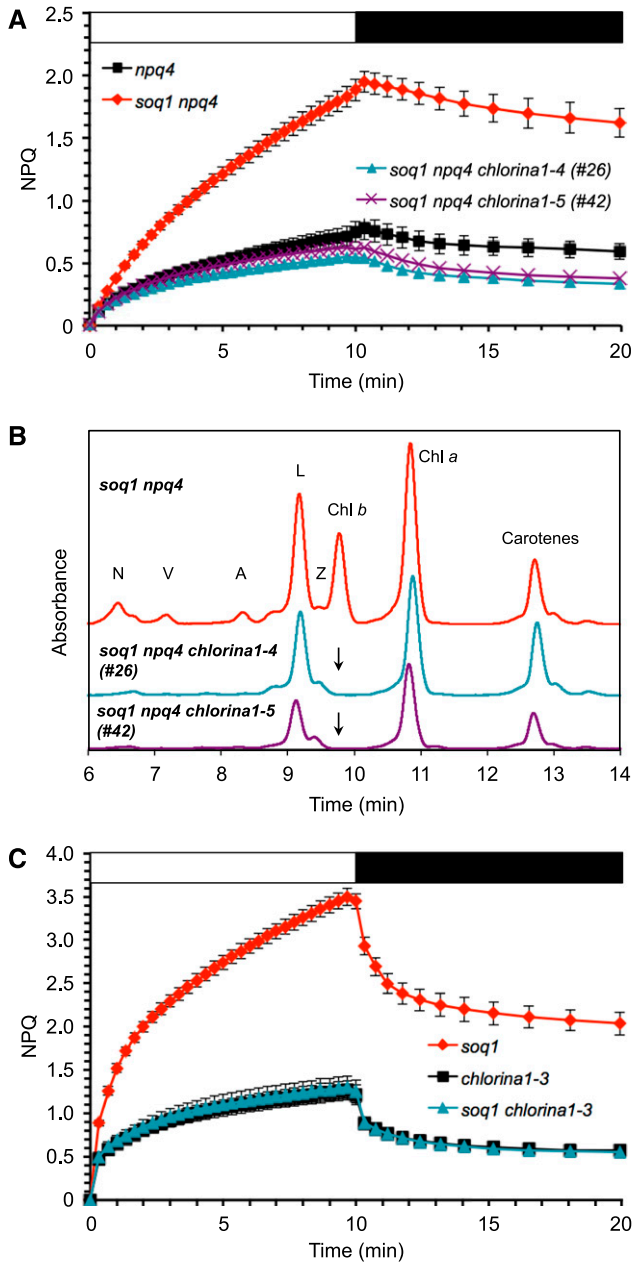

Figure 1. qH Requires Chlorophyll *b*.

(A) NPQ kinetics of *npq4*, *soq1 npq4*, and strict suppressors #26 and #42. Plants were grown at 120 μmol photons m^{-2} s^{-1}, induction of NPQ at 1200 μmol photons m^{-2} s^{-1} (white bar), and relaxation in the dark (black bar). **(B)** HPLC traces showing lack of chlorophyll *b* in mutants #26 and #42 (black arrow) after 1-h high-light treatment (1000 μmol photons m^{-2} s^{-1}) of detached leaves (pigments were extracted from same leaf area). N, neoxanthin; V, violaxanthin; A, antheraxanthin; Z, zeaxanthin; L, lutein; Chl, chlorophyll. **(C)** NPQ kinetics of *chlorina1-3* and *soq1 chlorina1-3*. The *soq1 chlorina1* mutant was identified among the F2 progeny of the cross *soq1-1* × *chlorina1-3*. Data represent means ± SD (n = 4 individuals). Plants were grown at 20 μmol photons m^{-2} s^{-1}, induction of NPQ at 2000 μmol photons m^{-2} s^{-1} (white bar), and relaxation in the dark (black bar). A *chlorina1* mutant has a smaller antenna size and one could argue that qH is not observed because light conditions are insufficient to trigger it in this mutant context. Lowest growth and highest induction light intensities were therefore chosen to maximize light differential. *soq1* NPQ kinetics (standard conditions, n = 3 individuals) is shown for reference.

#252 mutant, which contains an independent mutant allele of the gene of interest. Of the five genes containing mutations predicted to cause an amino acid change within the mapped region of #205, only one gene, At3g47860 encoding the chloroplastic lipocalin (CHL), now renamed plastid lipocalin (LCNP), was also mutated in #252 (Supplemental Table 2). Please note that we renamed this protein to avoid confusion with the abbreviation Chl that is commonly used for chlorophyll and to be consistent with the nomenclature used for the animal lipocalin family (LCN). Nucleotide transitions C to T and G to A resulted in Ala255Val in #205 and a mutated splice site in #252, respectively (Figure 3). We named these alleles *lcnp-2* and *lcnp-3* and accordingly named the knockout (KO) allele AtCHL KO (T-DNA SALK insertion line; described in Levesque-Tremblay et al., 2009) *lcnp-1*. We will use *lcnp* when referring to the latter line for clarity.

The Plastid Lipocalin Is Required for qH to Occur

We examined the NPQ phenotype of *lcnp* and found that it exhibited the same NPQ kinetics and amplitude as the wild type when grown under standard conditions and induced at 1200 μmol photons m^{-2} s^{-1} (Figure 2C, green curve). This result indicates that LCNP does not play a role in NPQ under these conditions. However, as evidenced by the two suppressor mutants #205 and #252, the additional NPQ observed in the *soq1 npq4* mutant relies on the presence of the LCNP protein. To confirm the involvement of LCNP in qH, we crossed the single *soq1* mutant to *lcnp*. The *soq1 lcnp* double mutant showed an NPQ phenotype similar to the wild type (Figure 2C, blue curve), which further validates the requirement of LCNP for qH to occur. The *soq1*/*soq1 lcnp*/*LCNP* strain showed NPQ kinetics intermediate to that of the *soq1* mutant and the wild type, which means that the *lcnp* mutation is semidominant (Figure 2C, orange curve). Similarly, as stated above, the mutation LCNP-Ala255Val in *lcnp-2* (#205) is semidominant in that the NPQ phenotype of the *soq1*/*soq1 npq4*/*npq4 lcnp-2*/*LCNP* strain is intermediate to that of *soq1 npq4* and *npq4* (Figure 2A, orange curve).

Immunoblot Analysis Shows That the Mobility of LCNP Is Altered in *soq1*

We probed the accumulation of the LCNP protein in the suppressor mutants by immunoblot analysis. The amino acid change in the *lcnp-2* allele resulted in the reduced accumulation of the protein (Figure 4A). The mutated splice site in *lcnp-3* resulted in the absence of LCNP (Figure 4A). Plants heterozygous for the *lcnp* mutation (*soq1*/*soq1 lcnp*/*LCNP*) contained intermediate amounts of LCNP protein (Figure 4B; Supplemental Figure 2). Interestingly, the apparent molecular mass of LCNP was slightly higher (~1.5 kD) in the *soq1* mutant background compared with the wild type (Figures 4A and B). This migration shift was also observed in the *lcnp-2* allele. Because SOQ1 contains a thioredoxin-like domain in the lumen, it is

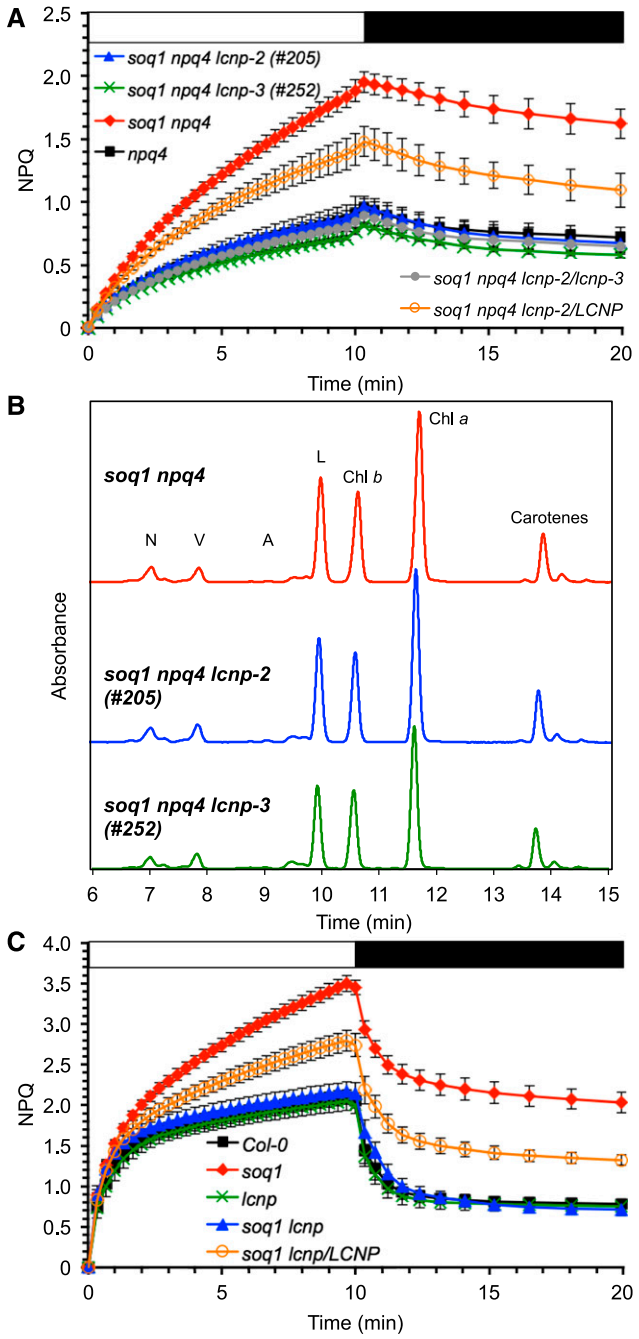

Figure 2. qH Requires the Plastid Lipocalin, LCNP.

(A) NPQ kinetics of *npq4*, *soq1 npq4*, strict suppressors #205 and #252, F1 from cross *soq1 npq4* x #205, and from cross *#205* x *#252*. Data represent means ± SD (n = 3 individuals).

(B) Representative HPLC traces from *soq1 npq4* and mutants #205 and #252 grown at 120 μmol photons m^{-2} s^{-1}. Pigments were extracted from same leaf area (n = 3 individuals). Total chlorophylls per area was compared among genotypes by Student's t test with $P < 0.01$; no significant difference was found. N, neoxanthin; V, violaxanthin; A, antheraxanthin; L, lutein; Chl, chlorophyll.

(C) NPQ kinetics of Col-0, *soq1*, *lcnp*, *soq1 lcnp*, and *soq1*/*soq1 lcnp*/*LCNP*. The *soq1 lcnp* mutant was identified among the F2 progeny of the cross *soq1-1* × *lcnp-1* (T-DNA knockout mutant). Data represent means ± SD (n = 3 for Col-0 and *soq1*, n = 6 for *lcnp*, n = 4 F2 individuals *soq1*/*soq1 lcnp*/*LCNP* and n = 7 F3 individuals *soq1 lcnp*). Growth at 120 μmol photons m^{-2} s^{-1}, induction of NPQ at 1200 μmol photons m^{-2} s^{-1} (white bar), and relaxation in the dark (black bar).

possible that SOQ1 maintains its target(s) in a reduced state (Brooks et al., 2013). LCNP is a soluble protein located in the lumen (Levesque-Tremblay et al., 2009) that contains six conserved cysteine residues (Figure 3). The altered mobility of LCNP in the *soq1* mutant background suggests that this protein could be an oxidized form of LCNP; however, it was not reversed by the addition of DTT, a reducing agent (Figure 4A). Attempts to determine the reason for this altered mobility have so far been unsuccessful. We tested whether it was a signature for active LCNP, but it does not seem to be the case, as LCNP in Col-0 still migrated differently from LCNP in *soq1* after a cold and high-light treatment (Figure 4B) that induces qH (see below). However, this altered mobility suggests that SOQ1 and LCNP function within a similar pathway at the biochemical level.

qH Operates in Cold and High Light Conditions

Both LCNP mRNA and protein expression increase during abiotic stresses such as high light and drought (Levesque-Tremblay et al., 2009). Interestingly, the *lcnp* mutant shows increased lipid peroxidation after a high-light (1300 μmol photons m^{-2} s^{-1}) and cold treatment (7°C) for 24 h (Levesque-Tremblay et al., 2009). We hypothesized that LCNP-dependent qH contributes to abiotic stress resistance and thus tested the induction of qH under cold and high light conditions in the different genotypes (Col-0, *lcnp*, *soq1*, and *soq1 lcnp*). Figure 5A (left panel) shows that all four lines grew similarly under standard growth conditions and presented no visible differences. Under control conditions, all four lines displayed similar minimal fluorescence, F_o, and maximal fluorescence, F_m, parameters (Figures 5B and 5C, left panel). However, after a 6-h cold (6°C) and high-light (1500 μmol photons m^{-2} s^{-1}) treatment, F_o and F_m values were significantly lower in Col-0 and *soq1* compared with *lcnp* and *soq1 lcnp* (Figures 5B and 5C, right panel). This experiment demonstrates that under cold and high-light stress, Col-0 displayed quenching of both F_m and F_o in an LCNP-dependent manner (Figures 5B and 5C, right panel Col-0 versus *lcnp*). Similarly, *soq1* displayed quenching of both F_m and F_o in an LCNP-dependent manner (Figures 5B and 5C, right panel *soq1* versus *soq1 lcnp*). Yet, *soq1* displayed a larger decrease in F_m compared with Col-0 (Figure 5C, right panel Col-0 versus *soq1*), which reveals the contribution of LCNP-dependent quenching during stress condition when its inhibitor, SOQ1, is no longer preventing quenching from occurring. These observed differences in fluorescence characteristics are due to the combination of both cold and high-light conditions, as a cold and standard light treatment did not lead to changes in F_m (Supplemental Figure 3B, right panel). We also confirmed that fluorescence differences are not due to altered chlorophyll content or deepoxidation state (A+Z)/(V+A+Z) (Supplemental Table 3).

The fluorescence phenotype induced by cold and high-light treatment of seedlings (Figure 5) was also observed at later growth stages in mature plants (Figure 6A). We repeated the cold and high-light experiment on detached leaves (Figure 6B;

Table 1. Pigment Content without or with Cold and High-Light Treatment

Genotype	Col-0	*soq1 lcnp/LCNP*	*soq1*	*lcnp*	*soq1 lcnp*	*npq4*	*soq1 npq4*	*soq1 npq4 lcnp-2*	*soq1 npq4 lcnp-3*	*npq4 lcnp-2*
Without treatment + 10 min dark acclimation										
Total chlorophyll (nmol cm^{-2})	31.0 ± 0.62	32.6 ± 3.3	32.5 ± 1.4	31.5 ± 1.2	30.1 ± 4.5	34.0 ± 2.3	31.9 ± 0.8	29.8 ± 1.0	37.9 ± 3.6	38.9 ± 8.6
Chlorophyll *a*/*b*	2.66 ± 0.04	2.62 ± 0.11	2.64 ± 0.03	2.68 ± 0.07	2.71 ± 0.14	2.67 ± 0.08	2.74 ± 0.03	2.69 ± 0.06	2.59 ± 0.06	2.67 ± 0.02
(A+Z)/(V+A+Z)	0.04 ± 0.01	0.04 ± 0	0.05 ± 0.01	0.02 ± 0.02	0.05 ± 0	0.04 ± 0	0.06 ± 0.02	0.07 ± 0.02	0.08 ± 0.01	0.07 ± 0.02
Cold and high-light treatment + 40 min dark acclimation										
Total chlorophyll (nmol cm^{-2})	25.7 ± 1.3	31.7 ± 5.3	25.2 ± 2.0	26.4 ± 1.1	29.0 ± 3.4	27.8 ± 4.8	26.7 ± 2.0	27.5 ± 4.3	29.6 ± 3.8	33.8 ± 4.7
Chlorophyll *a*/*b*	3.05 ± 0.21	3.15 ± 0.22	3.11 ± 0.12	2.77 ± 0.01	2.79 ± 0.04	2.98 ± 0.11	2.98 ± 0.23	2.92 ± 0.07	2.79 ± 0.14	2.76 ± 0.06
(A+Z)/(V+A+Z)	0.78 ± 0.03	0.71 ± 0.07	0.70 ± 0.01	0.71 ± 0.02	0.68 ± 0.03	0.73 ± 0.05	0.66 ± 0.09	0.69 ± 0.10	0.71 ± 0.07	0.62 ± 0.06

Pigments were extracted from leaves of plants grown in standard conditions, without or with exposure to cold and high-light conditions (5 h at 6°C and 1500 μmol photons m^{-2} s^{-1}) and dark-acclimated for 10 or 40 min, respectively. Data represent means ± sd (n = 3 leaves from different plant individuals).

Supplemental Figure 4) and calculated NPQ from the F_m values before treatment and after treatment plus a 10-min dark acclimation to relax qE (Figure 6C). Therefore, the measured NPQ represents the sum of slowly relaxing quenching components: qH, qZ, and qI. We confirmed the observations from the seedling experiment and found that in agreement with the semidominant nature of the *lcnp* mutation in the *soq1* background, the *soq1*/*soq1 lcnp*/*LCNP* line displayed intermediate F_m quenching between Col-0 and *soq1*. We also tested the cold and high light response in the original suppressor lines containing the *npq4* mutation and observed a similar trend as in the wild-type background: enhanced qH in *soq1 npq4* compared with *npq4* that required LCNP (*soq1 npq4 lcnp-3* lacks LCNP protein and, therefore, its NPQ value was equivalent to that of *lcnp*). Of note, *soq1 npq4 lcnp-2*, which contains a low amount of LCNP-Ala255Val, displayed some F_m quenching compared with *soq1 npq4 lcnp-3*. Similar to the seedling experiment, the chlorophyll content and deepoxidation state were equivalent among genotypes (Table 1; Supplemental Table 4). We compared the organization of thylakoid complexes by nondenaturing gel electrophoresis using the 25BTH20G method described by Järvi et al. (2011) to preserve the integrity of the membrane complexes and did not see any organizational differences among genotypes under conditions in which qH is on (cold high light) or off (growth light) (Supplemental Figure 5).

LCNP-Dependent Quenching qH Is Photoprotective

To further explain the stress sensitivity exhibited by the *lcnp* mutant under cold and high-light conditions (Levesque-Tremblay et al., 2009), we tested whether operation of qH is photoprotective by measuring lipid peroxidation levels. Lipid peroxidation autoluminescence imaging measures the faint light emitted by triplet carbonyls and $^1O_2$ by-products of the slow spontaneous decomposition of lipid hydroperoxides and endoperoxides (Havaux et al., 2006). A high value of autoluminescence corresponds to a high level of lipid peroxidation. Figures 7A and 7D confirm that, under the conditions used, LCNP-dependent NPQ was on, as demonstrated by the low F_m values in lines containing LCNP. In agreement with previously published data (Levesque-Tremblay et al., 2009), *lcnp* showed a high level of lipid peroxidation compared with Col-0 (Figure 7E). Importantly the *soq1* mutant displayed a lower level of lipid peroxidation compared with Col-0 (Figure 7B). We further quantified lipid peroxidation levels by measuring the concentration of oxidation products of linolenic acid, the major polyunsaturated fatty acid in plant leaves. Hydroxyoctadecatrienoic acid (HOTE) level was calculated as the sum of the various HOTE isomers (9-, 12-, 13-, and 16-HOTE). Both *soq1* and Col-0 had significantly lower levels of HOTE compared with *lcnp*, and *soq1* also had significantly lower levels of HOTE compared with Col-0 (Figures 7C and 7F).

Overexpression (OE) of LCNP has been shown to result in lower levels of lipid peroxidation (Levesque-Tremblay et al., 2009). We tested whether this was associated with increased NPQ, which was indeed the case, as *LCNP OE* displayed lower F_m than Col-0 (Figure 7A). Consequently, the low F_m value correlated (similarly to *soq1*) to low levels of lipid peroxidation and HOTE in *LCNP OE* (Figures 7B

Figure 3. Schematic Representation of LCNP Protein with Positions of the Mutations.

Predicted chloroplast transit peptide (cTP) and lumen transit peptide (ITP) based on software prediction for cTP and mass spectrometry data (from ppdb.tc.cornell.edu) for ITP suggesting a mature size of 29 kD; black squares, "structurally conserved regions" of the lipocalin fold; diamonds, conserved cysteines; adapted from (Charron et al., 2005). Positions of three mutant alleles are depicted: T-DNA KO mutant (*lcnp-1*) described by Levesque-Tremblay et al. (2009), LCNP-Ala255Val (*lcnp-2*), and splice site (*lcnp-3*) mutants from suppressor mutants #205 and #252, respectively, isolated in this study.

and 7C). Altogether, these results demonstrate that the LCNP-dependent qH quenching mechanism is photoprotective.

DISCUSSION

The molecular basis of sustained forms of energy dissipation is not well known. Previously, we identified a factor, SOQ1, that negatively regulates such a form of energy dissipation (Brooks et al., 2013), which we named qH. In the work reported here, we found a factor, LCNP, that is required for this form of energy dissipation to occur.

The Sustained NPQ Mechanism qH Depends on LCNP and Is Photoprotective

The plastid lipocalin, LCNP, is required for qH, as neither the triple mutants *soq1 npq4 lcnp-2* (#205) and *soq1 npq4 lcnp-3* (#252) (Figure 2A) nor the double mutant *soq1 lcnp* (Figure 2C) showed the additional quenching that is characteristic of *soq1*. LCNP has been previously shown to accumulate under drought and high-light stresses where it is thought to function in preventing or modulating singlet oxygen ($^1O_2$)-mediated lipid peroxidation (Levesque-Tremblay et al., 2009). We investigated whether the stress sensitivity exhibited by the *lcnp* mutant after cold and high light stress (Levesque-Tremblay et al., 2009) was due to the lack of the quenching mechanism enabled by LCNP. We indeed found that exposure to cold and high-light conditions results in sustained quenching of both F_o and F_m that is LCNP dependent (Figures 5 and 6; Supplemental Figure 4), indicating that LCNP-dependent qH quenching operates in the wild type under these conditions. LCNP-dependent quenching is equivalent to the difference in F_m level between the wild type and *lcnp* (see also Figure 6C for NPQ calculation). Furthermore, operation of qH is photoprotective, as shown by the decreased lipid peroxidation levels in both the wild type (Figure 7, Col-0) and mutants with enhanced qH (Figure 7, *soq1* and LCNP OE) when treated with cold and high light and by the reduced bleaching in response to this stress (Supplemental Figure 6). Levesque-Tremblay et al. (2009) proposed that LCNP manages peroxidized lipids by either detoxifying them or preventing their formation. NPQ has been proposed to mitigate $^1O_2$ production (Müller et al., 2001), and PsbS-dependent quenching has been shown to limit $^1O_2$ production (Roach and Krieger-Liszkay, 2012). Our study therefore suggests that the accumulation of peroxidized lipids observed in *lcnp* following abiotic stress is a consequence of the absence of the photoprotective NPQ mechanism enabled by LCNP and, thus, that LCNP might function in preventing the formation of peroxidized lipids. In addition to or as part of its role in NPQ, it is conceivable that LCNP might detoxify peroxidized lipids directly; this function would further contribute to decreasing levels of lipid peroxidation.

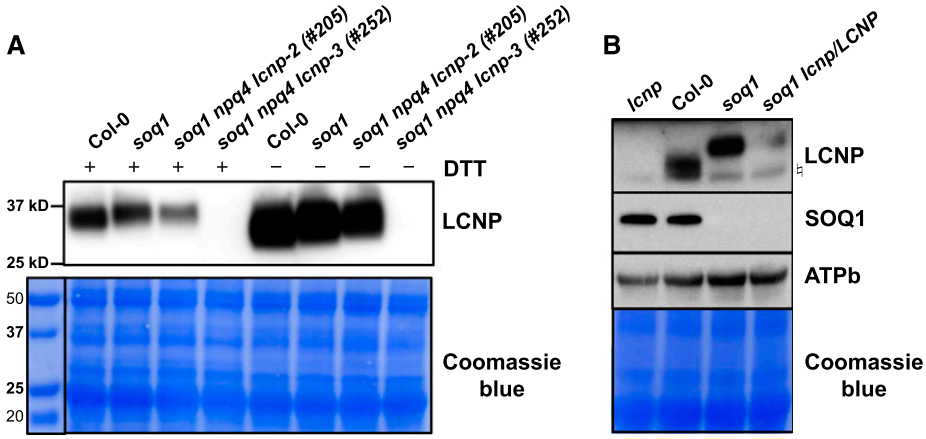

Figure 4. LCNP Protein Mobility Is Altered in the *soq1* Mutant Background.

Proteins were separated by SDS-PAGE and analyzed by immunodetection with antibodies against LCNP, SOQ1, or ATPb. Samples were loaded at the same chlorophyll content. Coomassie blue and/or ATPb are shown as loading controls.

(A) Isolated thylakoids ±100 mM DTT from plants grown under standard conditions (3.5 μg chlorophyll). Molecular masses (kD) are indicated according to the migration of Precision Plus Protein Standards markers from Bio-Rad.

(B) Isolated thylakoids (+100 mM DTT) from plants treated with cold and high light for 6 h at 6°C and 1500 μmol photons m^{-2} s^{-1} (5 μg chlorophyll). Symbol represents nonspecific band detected by the anti-LCNP antibody.

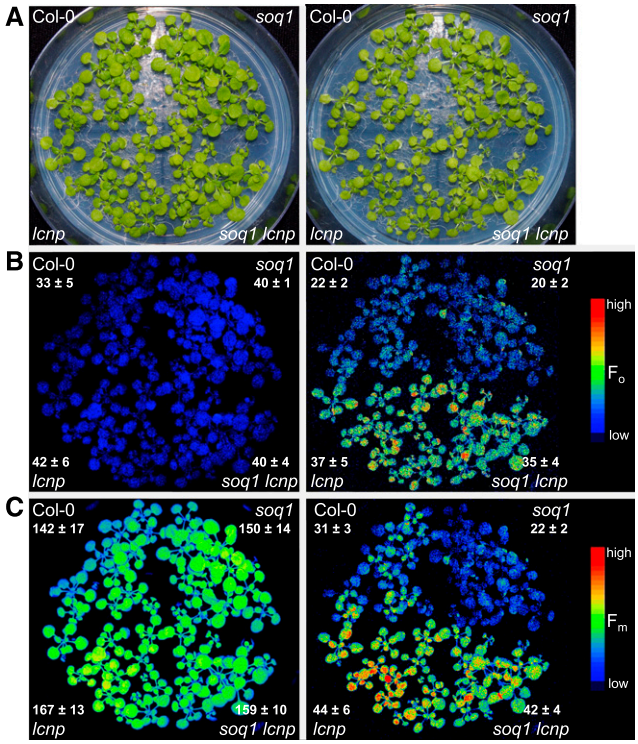

Figure 5. qH Occurs under Cold and High-Light Conditions (Seedlings).

Images of seedlings **(A)** and false-colored images of minimum fluorescence (F_o; **[B]**) and maximum fluorescence (F_m; **[C]**). Left panel: 24-d-old seedlings grown at 120 μmol photons m^{-2} s^{-1}, 21°C immediately before treatment. Right panel: after a cold and high-light treatment for 6 h at 6°C and 1500 μmol photons m^{-2} s^{-1}. Seedlings were dark-acclimated for 10 min before fluorescence measurement to relax qE. In **(B)** and **(C)**, right panel, color scale is expanded to better visualize differences. See Supplemental Figure 3 for nonexpanded color scale image of F_m. Average values and SD are given with $n = 9$ individuals for each genotype.

Function of LCNP in NPQ

The name of the lipocalin domain comes from the eight-stranded antiparallel beta sheet that forms a barrel or a calyx (cup-like structure) and its high affinity for small hydrophobic molecules. Proteins from the lipocalin family bind to or carry hydrophobic molecules such as retinoids, fatty acids, steroids, odorants, and pheromones or can have enzymatic activity, e.g., prostaglandin isomerase (Grzyb et al., 2006). A distinction is made between true lipocalins and lipocalin-like proteins based on the number of structurally conserved regions (SCR) they contain (Charron et al., 2005). LCNP belongs to the group of true lipocalins, as it contains three SCRs (Figure 3). In the Arabidopsis genome (or other land plants), there is another true lipocalin, TIL (for temperature-induced lipocalin; Frenette Charron et al., 2002), which locates to different cell membranes and organelles (but not the chloroplast), depending on growth conditions (Charron et al., 2005; Hernández-Gras and Boronat, 2015). TIL and LCNP play a role during abiotic stress and have overlapping functions in protecting against lipid peroxidation (Boca et al., 2014), but their mechanism of action is unknown. The first reported plant lipocalin-like proteins are the xanthophyll cycle enzymes VDE and ZEP (Bugos et al., 1998), which also play an important role in photoprotection (Niyogi et al., 1998). LCNP-dependent NPQ does not require zeaxanthin (Brooks et al., 2013), violaxanthin, or lutein (Supplemental Figures 7 to 9), so the known carotenoids involved in light harvesting or energy dissipation are unlikely to be the hydrophobic molecule that LCNP binds. Further experiments that aim at determining the ligand or substrate of LCNP will provide insights into its involvement in enabling this sustained form of energy dissipation.

Interestingly, heterozygotes for the mutation in *LCNP* in a *soq1* homozygote context showed an intermediate NPQ phenotype (Figures 2A, 2C, and 6C). This observation means that the yield of qH is sensitive to *LCNP* copy number and likely LCNP protein level. This semidominance could signify that LCNP has enzymatic activity and is rate-limiting for the reaction it catalyzes, as was proposed for PsbS and LUT2 based on heterozygotes of *npq4* (Li et al., 2000) and *lut2* (Pogson et al., 1996), mutations that show a similar dosage-dependent phenotype. Accordingly, the overexpression of LCNP resulted in higher NPQ than Col-0 (Figure 7A). Perhaps LCNP is the site of quenching itself, but its lumenal localization (even if it would be tethered to the membrane during quenching activity) seems to be incompatible, in terms of distance, with a hypothesized charge or energy transfer from the PSII peripheral antenna (see below). In either case, our results imply that there is a correlation between the yield of qH and the amount (or activity) of LCNP rather than LCNP being limited by a putative substrate. The variant LCNP-Ala255Val showed a lower accumulation of the protein (Figure 4A), which led to no induction of additional NPQ in the *soq1* mutant context during a 10-min light treatment (Figure 2A, blue curve). However after a 6-h cold and high-light treatment, some NPQ can be turned on (Figures 6B and 6C, *soq1 npq4 lcnp-2* compared with *soq1 npq4 lcnp-3*). Ala255Val destabilizes the LCNP protein and results in partial loss of function. Residue Ala-255 from AtLCNP shows 100% conservation among the eight sequences of LCNP homologs analyzed by Charron et al. (2005) and is located at the end of SCR2 (Figure 3), which is consistent with its impact on LCNP function.

The Site of qH Is in the Antenna of PSII

In our suppressor screen on *soq1 npq4*, we also identified two new mutant alleles affecting CAO, as demonstrated by the absence of chlorophyll *b* in the mutants #26 and #42 (Figure 1B) and confirmed by candidate gene sequencing. CAO is located in the chloroplast and catalyzes a two-step oxygenase reaction involved in the synthesis of chlorophyll *b* through its Rieske (2Fe2S cluster) and non-heme iron cofactors (Tanaka et al., 1998). The alleles described previously in Arabidopsis were obtained by x-ray mutagenesis. *chlorina1-1* is a null allele that accumulates a truncated form of the protein (415 amino acids out of 536). *chlorina1-2* is a leaky allele and contains an amino acid change Val274Glu within the 2Fe2S cluster binding site. *chlorina1-3* is a null allele with a deletion of 40 amino acids at the iron binding site. Through EMS mutagenesis, we found two additional alleles named *chlorina1-4* and *chlorina1-5*, which correspond to Gln89STOP and Thr375Ile, respectively. The truncated protein resulting from the early stop codon in *chlorina1-4* is likely to produce a nonfunctional protein. Thr-375 is a conserved amino acid (Tomitani et al., 1999) located in the vicinity of the iron binding site, suggesting that *chlorina1-5* is likely to affect catalytic

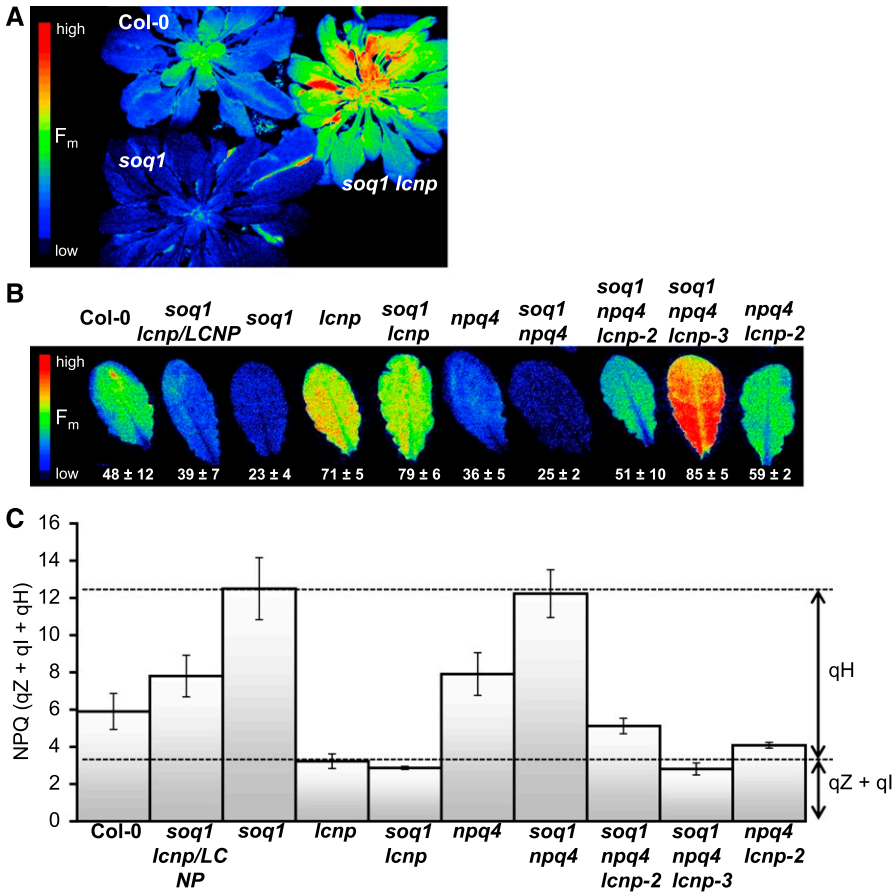

Figure 6. qH Occurs under Cold and High-Light Conditions (Whole Plants and Detached Leaves).

(A) and **(B)** Plants and leaves were dark-acclimated for 10 min before fluorescence measurement to relax qE. False-colored image of maximum fluorescence (F_m) from 7-week-old plants **(A)** and detached leaves from 6-week-old plants **(B)**, after a cold and high-light treatment for 5 h at 6°C and 1500 μmol photons m^{-2} s^{-1}.

(C) NPQ values from detached leaves experiment (see representative image shown in **[B]**) calculated as (F_m before treatment – F_m after treatment)/(F_m after treatment). Data represent means ± SD ($n = 3$ leaves from different plant individuals). The *lcnp-2* allele accumulates lower levels of mutated LCNP-Ala255Val; the *lcnp* and *lcnp-3* alleles accumulate no LCNP protein.

activity. As chlorophyll *b* was not detected in either *chlorina1-4* or *-5* (Figure 1B), it appears that they are both null alleles of CAO, which is consistent with the nature of the mutations.

The *soq1 npq4 chlorina1-4* and *-5* mutants displayed a low level of NPQ similar to that of *npq4* (Figure 1A); accordingly, *soq1 chlorina1-3* displayed the same level of NPQ as the *chlorina1-3* mutant (Figure 1C). A *chlorina1* mutant lacks oligomeric organization of Lhcb proteins such as trimeric LHCII and PSII-LHCII supercomplexes but still accumulates apo-monomeric Lhcb proteins (not containing chlorophyll) and monomeric Lhcb containing chlorophyll *a* (Espineda et al., 1999; Havaux et al., 2007; Takabayashi et al., 2011). The absence of oligomeric PSII peripheral antenna in a *soq1* mutant background abolishes the induction of additional quenching; therefore, we conclude that qH occurs in the oligomeric peripheral antenna of PSII. Future study will explore the specific antenna protein(s) that are necessary for qH. Lipid composition is known to modulate LHCII aggregation state and function (Schaller et al., 2011). It is possible that LCNP-mediated modification of a hydrophobic molecule, such as a thylakoid membrane lipid, would change the conformation of LHCII and thus create a quenching site. Interestingly, a potential biochemical interaction between wheat (*Triticum aestivum*) LCNP with the lipid transfer protein 3 and a β-ketoacyl-acyl carrier protein synthase involved in fatty acid synthesis was found by yeast two-hybrid analysis (using dehydrated plant cDNA libraries) (Tardif et al., 2007). These potential interactions and their relevance for LCNP function will be subjects of further examination.

Regulation of qH by SOQ1

The suppressor screen revealed a genetic interaction between SOQ1 and LCNP: Upon mutation of *LCNP* in a *soq1* mutant background (*soq1 lcnp*), qH was no longer induced (Figure 2C). Furthermore, under cold and high-light conditions, the wild type exhibited F_m and F_o quenching in an LCNP-dependent manner but to a lesser extent than

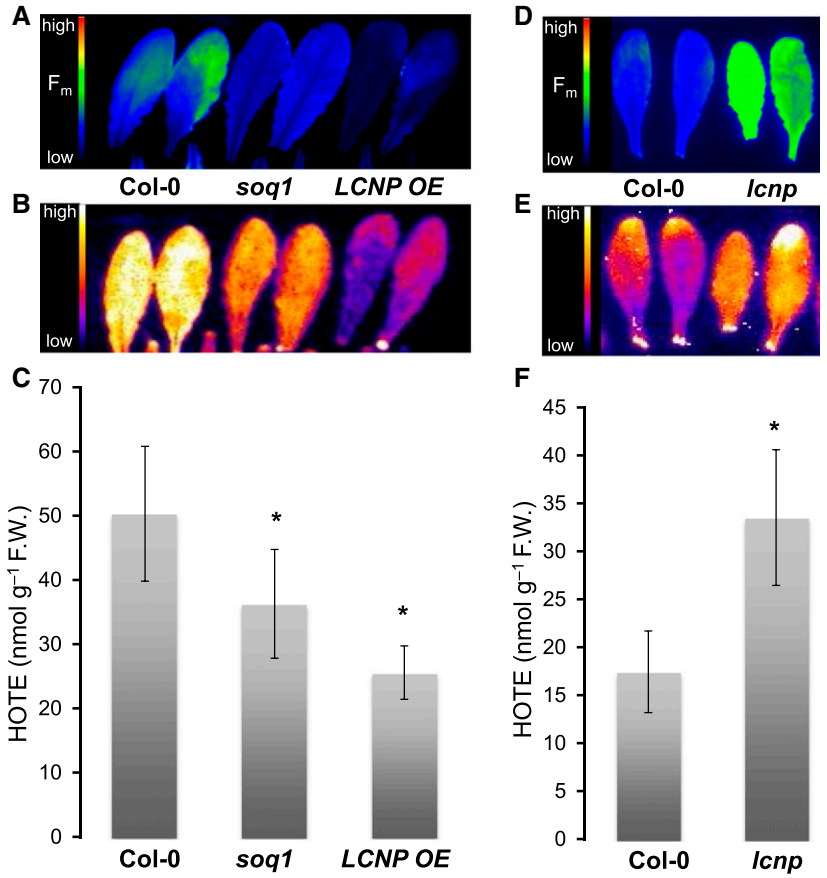

Figure 7. qH Is Photoprotective.

Leaves were exposed to cold and high-light treatment for 3 h (**[A]**, **[B]**, **[D]**, **[E]**, and **[F]**) or 6 h **(C)** at 6°C and 1500 μmol photons m^{-2} s^{-1}. Representative images of maximum chlorophyll fluorescence, (F_m; **[A]** and **[D]**) after a 10-min dark acclimation to relax qE and autoluminescence originating from lipid peroxides (**[B]** and **[E]**). This time point (3 h instead of 6 h) was chosen and *lcnp* was measured separately to prevent saturation and drowning out of the luminescence signal between genotypes with lower lipid peroxidation levels than Col-0. Camera settings in **(B)** were adjusted to better visualize differences. In **(C)** and **(F)**, quantification of lipid peroxidation is expressed as HOTE level. The 6 h time point in **(C)** was chosen for consistency with the time point used in Figure 5. Data represent means ± SD (n = 3 samples of pooled leaves from six individuals). Asterisks mark significant difference relative to Col-0 at $P < 0.05$ by Student's t test.

soq1 (Figures 5 and 6). These results demonstrate that LCNP is required for qH as discussed above and that the function of SOQ1 is to inhibit (quenching by) LCNP. Alternatively, SOQ1 could be involved in removing or recycling the quenching sites that are enabled by LCNP, but we do not favor this idea for several reasons. As LCNP is located in the thylakoid lumen (Levesque-Tremblay et al., 2009), it is a good candidate for interacting with the SOQ1 domains responsible for regulating qH, namely, the thioredoxin-like and NHL-beta propeller domains (Brooks et al., 2013). A similar biochemical pathway is also suggested by the altered mobility of LCNP in the *soq1* mutant (Figure 4). This altered mobility of ~1.5 kD is not affected by mutation Ala255Val and is not reversed by the addition of a reducing agent such as DTT. These results suggest that this is not a redox modification or that it is a stable modification (such as cysteine sulfinic/sulfonic acid or oxidized methionine) that cannot be reversed by DTT. The altered mobility of LCNP in *soq1* suggests that SOQ1 is required to reverse this slower migrating form. Whether the interaction between SOQ1 and LCNP is direct or indirect will be tested in the future.

SOQ1 is downregulated during drought stress, as summarized by Noctor et al. (2014). This represents a possible way to alleviate the inhibition of LCNP during abiotic stresses by repressing the inhibitor. However, the *soq1* mutation is recessive, which might mean that a low level of SOQ1 protein is sufficient for its function. This leads us to think that the repression of qH by SOQ1 might be more complex than a binary system in which less of the repressor means more active target. *LCNP* and *SOQ1* genes are conserved among all land plants with sequenced genomes, including evergreens such as Norway spruce (*Picea abies*) (Nystedt et al., 2013), so it is possible that this quenching mechanism and its regulation are broadly conserved.

Physiological Relevance of a ΔpH-Independent Quenching Mechanism

Research by Dall'Osto et al. (2005) provided evidence for a ΔpH-independent quenching mechanism in plants that was later

termed qZ (Nilkens et al., 2010) because it relies on the presence of zeaxanthin. This mechanism is independent of PsbS and is based on the conformational change of (at least) the minor antenna protein CP26. In our study, after a cold and high-light treatment, we observed a decrease in F_m (or NPQ level of ~3) in all genotypes regardless of the presence or absence of LCNP (Figure 6C; Supplemental Figure 3B, middle panel). We measured the zeaxanthin content remaining after dark acclimation and found high and similar levels of zeaxanthin and deepoxidation states in all genotypes (Table 1; Supplemental Tables 3 and 4). Therefore, it is likely that some of this LCNP-independent NPQ level or decrease in F_m is due to qZ in addition to qI from photodamage and possibly other slowly relaxing processes.

LCNP-dependent NPQ does not depend on ΔpH, and this characteristic might provide a fitness advantage under specific environmental conditions. In Arabidopsis, we present evidence that qH is induced in the wild type during cold plus high-light stress (Figures 5 to 7). Dall'Osto et al. (2005) suggested that qZ could be responsible for part of the sustained ΔpH-independent quenching mechanism observed in overwintering evergreens (Verhoeven et al., 1999; Gilmore and Ball, 2000). A highly efficient quenching is necessary to enable overwintering evergreens to withstand extended periods of high light and cold (Adams et al., 2002; Öquist and Huner, 2003). We previously discussed the possibility that the SOQ1-related (Brooks et al., 2013) or LCNP-dependent qH further described here plays a role in this sustained form of NPQ. Tropical evergreens have also been shown to induce a sustained form of NPQ upon transition from shade to high light (Demmig-Adams et al., 2006), and it is likely that many plants need sustained quenching mechanisms to survive periods of extended light stress (Demmig-Adams and Adams, 2006). In the future, it would be interesting to test whether qZ or qH is the dominant form of energy dissipation in this sustained mode of photoprotection in other plant species. With the recent advances in gene editing technology in non-model organisms (Woo et al., 2015), knockout of *LCNP* in an evergreen species would be a direct way to test the contribution of LCNP to sustained photoprotection.

METHODS

Plant Material and Growth Conditions

Wild-type *Arabidopsis thaliana* and the derived mutants studied here are of the Col-0 ecotype. Mutants *npq4-1* (Li et al., 2000), *soq1-1*, *soq1 npq4 glabrous (gl)1-1* (Brooks et al., 2013), and *soq1-1 npq2-1* (Brooks, 2012) were previously isolated in our laboratory. The *lut2-2* (Pogson et al., 1996) mutant allele was crossed with *soq1-1*. We refer to the *npq4-1* and *soq1-1* mutant alleles as *npq4* and *soq1*, respectively, because no other mutant alleles of these genes were used in this study. Mutant *chlorina1-3 lhcb5* (Kim et al., 2009) was used as the source of the *chlorina1-3* allele. Mutants *soq1 npq4 gl1 chlorina1-4*, *soq1 npq4 gl1 chlorina1-5*, *soq1 npq4 gl1 lcnp-2*, and *soq1 npq4 gl1 lcnp-3* were generated in this study. The *lcnp* T-DNA insertion line SALK_133049C was provided by F. Ouellet (Université du Québec à Montréal). Plants were grown in soil (Sunshine Mix 4/LA4 potting mix; Sun Gro Horticulture Distribution) under a 10/14-h light/dark photoperiod at 120 μmol photons m^{-2} s^{-1}, unless stated otherwise, at 21°C for 5 to 6 weeks or on agar plates containing 0.5× Murashige and Skoog medium (VWR Scientific; 95026-314) at 100 μmol photons m^{-2} s^{-1} (continuous light) at 21°C and then transferred to soil. For the cold and high-light treatment, seedlings, plants, or detached leaves were placed for 6 h at 6°C and at 1500 μmol photons m^{-2} s^{-1} using a custom-designed LED panel built by JBeamBio with cool white LEDs BXRA-56C1100-B-00 (Farnell). Light bulbs used in the growth chambers were cool white (4100K) from Philips (F25T8/TL841 25W) for plants grown in soil and from General Electric (F17T8/SP41 17 W) for seedlings grown on agar plates.

Genetic Crosses and Genotyping Primers

Genetic crosses were done using standard techniques (Weigel and Glazebrook, 2006). A Phire Plant Direct PCR kit (ThermoFisher Scientific) was used for genotyping with the dilution protocol. Genotyping of the *soq1-1* allele was done either by sequencing of an 800-bp PCR product amplified with primers MDB74 forward (TAGGTGTGCCTACCAGCGAG) and MDB72 reverse (TGAGCCACCAGTGAGAATGTC) surrounding the point mutation, position G372 to A in mutant, or by amplifying a 248-bp product with dCAPS primers (Neff et al., 2002) AM145 forward (GAAGTGGTTTCTTTTGTACAATTCTGCA) and AM146 reverse (CAATACGAATAGCGCACACG), which is digested by *Pst*I if it is a wild-type allele. To genotype the *lcnp* T-DNA allele, AM164 forward (LP) (CCGCTTTGACATTTACATTACG) and AM165 reverse (RP) (TATAGCAATGTCGGCTCCAAC) were used with LBb1.3 to amplify a 569-bp product in the wild type (LP+RP), an 869-bp (with insert) product in *lcnp* (LBb1.3+RP) or both in heterozygous individuals according to the Salk Institute Genomic Analysis Laboratory T-DNA primer design tool.

EMS Mutagenesis and Screening of Suppressor Mutants

M2 seedlings were derived from mutagenesis of *soq1 npq4 gl1* seeds with 0.24% (v/v) EMS. Suppressors of *soq1 npq4* were screened based on their NPQ phenotype by chlorophyll fluorescence video imaging using an Imaging-PAM Maxi (Walz). For mutant screening, 60 to 80 seeds were plated per agar plate and 3-week-old seedlings were dark-acclimated for 20 min prior to measurement. NPQ was induced by 1000 μmol photons m^{-2} s^{-1} (blue actinic light) for 10 min and relaxed in the dark for 10 min.

Mutation Mapping and Identification by Whole-Genome Sequencing

To identify the mutation of interest, the mutant #205 (*soq1 npq4 gl1 lcnp-2*) was crossed to the *soq1 npq4 gl1* parental line, which was used to generate the EMS population. Plants displaying the mutant phenotype (low NPQ) in the F2 generation were identified and pooled for DNA extraction. Genomic DNA was extracted from F2 mutant plants from the cross *soq1 npq4 gl1* x #205 (pool of 75 seedlings), *soq1 npq4 gl1* (150 seedlings), and #252 M3 mutant pool (200 seedlings) using a Gentra Puregene kit (Qiagen). Genomic DNA was submitted to the Functional Genomics Laboratory (UC Berkeley) for preparation of the sequencing libraries, which were sequenced at the Vincent J. Coates Genomics Sequencing Laboratory (UC Berkeley). The three samples were multiplexed and run with an unrelated sample in two lanes on an Illumina HiSeq 2000/2500 to obtain 100-bp paired-end reads. The sequencing reads were mapped to the Col-0 reference genome (TAIR) and SNPs were detected using the CLC Genomics Workbench software. The SNPs present in the *soq1 npq4 gl1* background were subtracted from those identified in mutant #205 to identify SNPs likely to have been induced by this new round of EMS mutagenesis and therefore to be segregating in the mapping population. The SNPs were further filtered by coverage (between 20 and 200×), observed frequency (>25%), and mapping quality. The allelic frequency of each SNP in the pooled #205 mutant F2 was then plotted relative to the genomic position (Supplemental Figure 1) to identify the region showing linkage to the causative mutation. The set

of genes containing an amino acid changing mutation within this region for the #205 pool was then compared with the genes containing mutations in the #252 mutant.

Chlorophyll Fluorescence Measurement

Chlorophyll fluorescence was measured at room temperature from attached, fully expanded rosette leaves or leaf discs of same area using a Dual-PAM-100 (Walz) fluorimeter. Plants were dark-acclimated for 20 min and NPQ was induced by 1200 μmol photons m^{-2} s^{-1} (red actinic light) for 10 min and relaxed in the dark for 10 min unless stated otherwise. Maximum fluorescence levels after dark acclimation (F_m) and throughout measurement (F_m') were recorded after applying a saturating pulse of light. NPQ was calculated as ($F_m - F_m$')/F_m'. For the cold and high-light experiments shown in Figures 5 to 7, fluorescence was acquired with an Imaging-PAM Maxi from Walz and a JBeamBio fluorescence imaging setup (Johnson et al., 2009), respectively.

Protein Extraction and Immunoblot Analysis

Thylakoids were isolated as described (Iwai et al., 2015) and solubilized at 70°C for 4 min in 60 mM Tris HCl (pH 6.8), 2% SDS, and 6% sucrose with or without 100 mM DTT. For immunoblots, samples were loaded by chlorophyll content on anyKD gels (Bio-Rad), separated by SDS-PAGE, transferred in a semidry blotting apparatus at 0.8 mA cm^{-2} for 1 h to a PVDF membrane, blocked with 3% (w/v) nonfat dry milk, and incubated with the following antibodies. Rabbit-specific antibodies against a C-terminal peptide of SOQ1 (TVTPRAPDAGGLQLQGTR) were produced and purified by peptide affinity by ThermoFisher and used at a 1:2000 dilution. Anti-LCNP antibody against recombinant protein (Levesque-Tremblay et al., 2009) was provided by F. Ouellet (Université du Québec à Montréal) and used at a 1:2000 dilution. After incubation with HRP-conjugated secondary antibody, bands were detected by chemiluminescence with ECL substrate (GE Healthcare).

Pigment Extraction and Analysis

HPLC analysis of carotenoids and chlorophylls was done as previously described (Müller-Moulé et al., 2002). For the cold and high-light treatments, pigments were extracted from the same seedlings used in the fluorescence measurements shown in Figure 5 (two samples from different individuals per genotype per time point) or from the same plants used in the fluorescence measurements shown in Figure 6 (three samples from different individuals per genotype per time point).

Autoluminescence Imaging

Lipid peroxidation was visualized in leaves by autoluminescence imaging (Havaux et al. 2006). Leaves were dark acclimated for 2 h, and the luminescence emitted from the spontaneous decomposition of lipid peroxides was captured by a highly sensitive liquid N_2-cooled CCD camera, as previously described (Birtic et al., 2011). The images were treated using Image J software (NIH).

Lipid Peroxidation Analyses

Leaves (~0.5 g) were ground in an equivolume mixture of methanol/chloroform containing 5 mM triphenyl phosphine (PO3) and 1 mM 2,6-tert-butyl-*p*-cresol (5 mL g^{-1} fresh weight) and citric acid (2.5 mL g^{-1} fresh weight), using an Ultraturax blender. 15-HEDE was added as an internal standard to a final concentration 100 nmol g^{-1} fresh weight and mixed thoroughly. After centrifugation at 700 rpm and 4°C for 5 min, the lower organic phase was carefully taken out using a glass syringe and transferred into a 15-mL glass tube. The syringe was rinsed with ~2.5 mL chloroform and emptied into the tube containing the upper organic phase. The process was repeated and the lower layer was again collected and pooled with the first collected fraction. The solvent was evaporated under N_2 gas at 40°C. The residues were recovered in 1.25 mL absolute ethanol and 1.25 mL of 3.5 N NaOH and hydrolyzed at 80°C for 30 min. The ethanol was evaporated under N_2 gas at 40°C for ~10 min. After cooling to room temperature, pH was adjusted to 4 to 5 with 2.1 mL citric acid. Hydroxy fatty acids were extracted with hexane/ether 50/50 (v/v). The organic phase was analyzed by normal-phase HPLC-UV, as previously described (Montillet et al., 2004). HOTE isomers (9-, 12-, 13-, and 16-HOTE) derived from the oxidation of the main fatty acid, linolenic acid, were quantified based on the 15-HEDE internal standard.

Accession Numbers

Sequence data from this article can be found in the Arabidopsis Genome Initiative under accession numbers At1g56500 (SOQ1), At3g47860 (previously named CHL, renamed LCNP), At1g44575 (PsbS), and At1g44446 (CAO). Illumina HiSeq data can be found in the Sequence Read Archive (https://www.ncbi.nlm.nih.gov/sra) under BioProject number PRJNA420599 and BioSample numbers SAMN08116650 (*soq1 npq4 gl1*), SAMN08116641 (#205 F2), and SAMN08116657 (#252 M3).

Supplemental Data

Supplemental Figure 1. The causative mutation in mutant #205 is on chromosome 3.

Supplemental Figure 2. LCNP protein mobility is altered in the *soq1* mutant background.

Supplemental Figure 3. Cold and low-light treatment does not induce qH.

Supplemental Figure 4. F_m versus F_o values before and after cold and high-light treatment in detached leaves.

Supplemental Figure 5. The organization of the photosynthetic complexes upon cold and high-light treatment is similar among genotypes.

Supplemental Figure 6. qH is photoprotective.

Supplemental Figure 7. qH can occur in the absence of violaxanthin.

Supplemental Figure 8. qH can occur in the absence of lutein.

Supplemental Figure 9. qH can occur in the absence of both zeaxanthin and lutein.

Supplemental Table 1. Sequencing and reads mapping summary.

Supplemental Table 2. Summary of the identified mutations within the mapped region.

Supplemental Table 3. Pigment content in leaves from seedlings.

Supplemental Table 4. Pigment content in detached leaves.

ACKNOWLEDGMENTS

We thank Matthew Brooks, Lauriebeth Leonelli, and Phoi Tran for technical advice and assistance, Carine Marshall for advice regarding DNA sequencing, François Ouellet for providing antibodies against LCNP, Klaas van Wijk for non-public data from the Plant Proteome Database, Jean Alric for fluorescence measurement, Brigitte Ksas for help with the HOTE analyses, and Setsuko Wakao for critical reading of the manuscript. We also thank Robert Calderon, Laura Hug, and Cynthia Amstutz for critical discussions. We would like to dedicate this manuscript to the late Fabrice Rappaport

who will always be in our hearts and minds as we pursue the "bouleversifiant" endeavor of science. This research was supported by the Division of Chemical Sciences, Geosciences, and Biosciences, Office of Basic Energy Sciences, Office of Science, U.S. Department of Energy (Field Work Proposal 449B). This work used the Vincent J. Coates Genomics Sequencing Laboratory at UC Berkeley, supported by NIH S10 Instrumentation Grants S10RR029668 and S10RR027303. A.S. was supported by an NIH National Research Service Award Trainee appointment (grant GM007127). K.K.N. is an investigator of the Howard Hughes Medical Institute.

AUTHOR CONTRIBUTIONS

A.M. and K.K.N. designed research. A.M. performed research. A.S. performed bioinformatics analysis to identify the mutated gene. S.S. assisted with screening, planting, and seed collection. D.R. and M.H. performed lipid peroxidation experiments. A.M., D.R., M.H., and K.K.N. analyzed data. A.M. and K.K.N. wrote the article.

Received July 7, 2017; revised November 1, 2017; accepted December 8, 2017; published December 12, 2017.

REFERENCES

Adams III, W.W., Demmig-Adams, B., Rosenstiel, T.N., Brightwell, A.K., and Ebbert, V. (2002). Photosynthesis and photoprotection in overwintering plants. Plant Biol. **4:** 545–557.

Birtic, S., Ksas, B., Genty, B., Mueller, M.J., Triantaphylidès, C., and Havaux, M. (2011). Using spontaneous photon emission to image lipid oxidation patterns in plant tissues. Plant J. **67:** 1103–1115.

Boca, S., Koestler, F., Ksas, B., Chevalier, A., Leymarie, J., Fekete, A., Mueller, M.J., and Havaux, M. (2014). *Arabidopsis* lipocalins AtCHL and AtTIL have distinct but overlapping functions essential for lipid protection and seed longevity. Plant Cell Environ. **37:** 368–381.

Brooks, M.D. (2012). A Suppressor of Quenching Regulates Photosynthetic Light Harvesting. PhD dissertation (University of California, Berkeley).

Brooks, M.D., Sylak-Glassman, E.J., Fleming, G.R., and Niyogi, K.K. (2013). A thioredoxin-like/β-propeller protein maintains the efficiency of light harvesting in Arabidopsis. Proc. Natl. Acad. Sci. USA **110:** E2733–E2740.

Bugos, R.C., Hieber, A.D., and Yamamoto, H.Y. (1998). Xanthophyll cycle enzymes are members of the lipocalin family, the first identified from plants. J. Biol. Chem. **273:** 15321–15324.

Cazzaniga, S., Dall'Osto, L., Kong, S.G., Wada, M., and Bassi, R. (2013). Interaction between avoidance of photon absorption, excess energy dissipation and zeaxanthin synthesis against photooxidative stress in Arabidopsis. Plant J. **76:** 568–579.

Charron, J.B., Ouellet, F., Pelletier, M., Danyluk, J., Chauve, C., and Sarhan, F. (2005). Identification, expression, and evolutionary analyses of plant lipocalins. Plant Physiol. **139:** 2017–2028.

Chow, W.S., Osmond, C.B., and Huang, L.K. (1989). Photosystem II function and herbicide binding sites during photoinhibition of spinach chloroplasts in-vivo and in-vitro. Photosynth. Res. **21:** 17–26.

Dall'Osto, L., Caffarri, S., and Bassi, R. (2005). A mechanism of nonphotochemical energy dissipation, independent from PsbS, revealed by a conformational change in the antenna protein CP26. Plant Cell **17:** 1217–1232.

Demmig, B., and Björkman, O. (1987). Comparison of the effect of excessive light on chlorophyll fluorescence (77K) and photon yield of O_2 evolution in leaves of higher plants. Planta **171:** 171–184.

Demmig, B., Winter, K., Krüger, A., and Czygan, F.C. (1987). Photoinhibition and zeaxanthin formation in intact leaves : a possible role of the xanthophyll cycle in the dissipation of excess light energy. Plant Physiol. **84:** 218–224.

Demmig-Adams, B., and Adams III, W.W. (2006). Photoprotection in an ecological context: the remarkable complexity of thermal energy dissipation. New Phytol. **172:** 11–21.

Demmig-Adams, B., Ebbert, V., Mellman, D.L., Mueh, K.E., Schaffer, L., Funk, C., Zarter, C.R., Adamska, I., Jansson, S., and Adams, W.W. (2006). Modulation of PsbS and flexible vs sustained energy dissipation by light environment in different species. Physiol. Plant. **127:** 670–680.

Demmig-Adams, B., Koh, S.-C., Cohu, C.M., Muller, O., Stewart, J.J., and Adams III, W.W. (2014). Non-photochemical fluorescence quenching in contrasting plant species and environments. In Non-Photochemical Quenching and Energy Dissipation in Plants, Algae and Cyanobacteria, B. Demmig-Adams, G. Garab, W. Adams III, and Govindjee, eds (Dordrecht, The Netherlands: Springer), pp. 531–552.

Edelman, M., and Mattoo, A.K. (2008). D1-protein dynamics in photosystem II: the lingering enigma. Photosynth. Res. **98:** 609–620.

Espineda, C.E., Linford, A.S., Devine, D., and Brusslan, J.A. (1999). The *AtCAO* gene, encoding chlorophyll *a* oxygenase, is required for chlorophyll *b* synthesis in *Arabidopsis thaliana.* Proc. Natl. Acad. Sci. USA **96:** 10507–10511.

Frenette Charron, J.B., Breton, G., Badawi, M., and Sarhan, F. (2002). Molecular and structural analyses of a novel temperature stress-induced lipocalin from wheat and *Arabidopsis.* FEBS Lett. **517:** 129–132.

Gilmore, A.M., and Ball, M.C. (2000). Protection and storage of chlorophyll in overwintering evergreens. Proc. Natl. Acad. Sci. USA **97:** 11098–11101.

Grzyb, J., Latowski, D., and Strzałka, K. (2006). Lipocalins - a family portrait. J. Plant Physiol. **163:** 895–915.

Havaux, M., Triantaphylidès, C., and Genty, B. (2006). Autoluminescence imaging: a non-invasive tool for mapping oxidative stress. Trends Plant Sci. **11:** 480–484.

Havaux, M., Dall'osto, L., and Bassi, R. (2007). Zeaxanthin has enhanced antioxidant capacity with respect to all other xanthophylls in *Arabidopsis* leaves and functions independent of binding to PSII antennae. Plant Physiol. **145:** 1506–1520.

Hernández-Gras, F., and Boronat, A. (2015). A hydrophobic proline-rich motif is involved in the intracellular targeting of temperature-induced lipocalin. Plant Mol. Biol. **88:** 301–311.

Hirono, Y., and Redei, G.P. (1963). Multiple allelic control of chlorophyll *b* level in *Arabidopsis thaliana.* Nature **197:** 1324–1325.

Horton, P., Ruban, A.V., and Walters, R.G. (1996). Regulation of light harvesting in green plants. Annu. Rev. Plant Physiol. Plant Mol. Biol. **47:** 655–684.

Iwai, M., Yokono, M., Kono, M., Noguchi, K., Akimoto, S., and Nakano, A. (2015). Light-harvesting complex Lhcb9 confers a green alga-type photosystem I supercomplex to the moss *Physcomitrella patens*. Nat. Plants **1:** 14008.

Järvi, S., Suorsa, M., Paakkarinen, V., and Aro, E.M. (2011). Optimized native gel systems for separation of thylakoid protein complexes: novel super- and mega-complexes. Biochem. J. **439:** 207–214.

Johnson, M.P., and Ruban, A.V. (2011). Restoration of rapidly reversible photoprotective energy dissipation in the absence of PsbS protein by enhanced DeltapH. J. Biol. Chem. **286:** 19973–19981.

Johnson, X., Vandystadt, G., Bujaldon, S., Wollman, F.A., Dubois, R., Roussel, P., Alric, J., and Béal, D. (2009). A new setup for in vivo fluorescence imaging of photosynthetic activity. Photosynth. Res. **102:** 85–93.

Kim, E.H., Li, X.P., Razeghifard, R., Anderson, J.M., Niyogi, K.K., Pogson, B.J., and Chow, W.S. (2009). The multiple roles of light-harvesting chlorophyll a/b-protein complexes define structure and

optimize function of *Arabidopsis* chloroplasts: a study using two chlorophyll *b*-less mutants. Biochim. Biophys. Acta **1787:** 973–984.

Krause, G., Vernotte, C., and Briantais, J.-M. (1982). Photoinduced quenching of chlorophyll fluorescence in intact chloroplasts and algae. Resolution into two components. Biochim. Biophys. Acta **679:** 116–124.

Krause, G.H. (1988). Photoinhibition of photosynthesis. An evaluation of damaging and protective mechanisms. Physiol. Plant. **74:** 566–574.

Lambrev, P.H., Miloslavina, Y., Jahns, P., and Holzwarth, A.R. (2012). On the relationship between non-photochemical quenching and photoprotection of photosystem II. Biochim. Biophys. Acta **1817:** 760–769.

Levesque-Tremblay, G., Havaux, M., and Ouellet, F. (2009). The chloroplastic lipocalin AtCHL prevents lipid peroxidation and protects *Arabidopsis* against oxidative stress. Plant J. **60:** 691–702.

Li, X.P., Björkman, O., Shih, C., Grossman, A.R., Rosenquist, M., Jansson, S., and Niyogi, K.K. (2000). A pigment-binding protein essential for regulation of photosynthetic light harvesting. Nature **403:** 391–395.

Li, Z., Ahn, T.K., Avenson, T.J., Ballottari, M., Cruz, J.A., Kramer, D.M., Bassi, R., Fleming, G.R., Keasling, J.D., and Niyogi, K.K. (2009a). Lutein accumulation in the absence of zeaxanthin restores nonphotochemical quenching in the *Arabidopsis thaliana npq1* mutant. Plant Cell **21:** 1798–1812.

Li, Z., Wakao, S., Fischer, B.B., and Niyogi, K.K. (2009b). Sensing and responding to excess light. Annu. Rev. Plant Biol. **60:** 239–260.

Montillet, J.L., Cacas, J.L., Garnier, L., Montané, M.H., Douki, T., Bessoule, J.J., Polkowska-Kowalczyk, L., Maciejewska, U., Agnel, J.P., Vial, A., and Triantaphylidès, C. (2004). The upstream oxylipin profile of *Arabidopsis thaliana*: a tool to scan for oxidative stresses. Plant J. **40:** 439–451.

Müller, P., Li, X.P., and Niyogi, K.K. (2001). Non-photochemical quenching. A response to excess light energy. Plant Physiol. **125:** 1558–1566.

Müller-Moulé, P., Conklin, P.L., and Niyogi, K.K. (2002). Ascorbate deficiency can limit violaxanthin de-epoxidase activity *in vivo.* Plant Physiol. **128:** 970–977.

Neff, M.M., Turk, E., and Kalishman, M. (2002). Web-based primer design for single nucleotide polymorphism analysis. Trends Genet. **18:** 613–615.

Nilkens, M., Kress, E., Lambrev, P., Miloslavina, Y., Müller, M., Holzwarth, A.R., and Jahns, P. (2010). Identification of a slowly inducible zeaxanthin-dependent component of non-photochemical quenching of chlorophyll fluorescence generated under steady-state conditions in *Arabidopsis.* Biochim. Biophys. Acta **1797:** 466–475.

Niyogi, K.K., Björkman, O., and Grossman, A.R. (1997). The roles of specific xanthophylls in photoprotection. Proc. Natl. Acad. Sci. USA **94:** 14162–14167.

Niyogi, K.K., Grossman, A.R., and Björkman, O. (1998). *Arabidopsis* mutants define a central role for the xanthophyll cycle in the regulation of photosynthetic energy conversion. Plant Cell **10:** 1121–1134.

Noctor, G., Mhamdi, A., and Foyer, C.H. (2014). The roles of reactive oxygen metabolism in drought: not so cut and dried. Plant Physiol. **164:** 1636–1648.

Nystedt, B., et al. (2013). The Norway spruce genome sequence and conifer genome evolution. Nature **497:** 579–584.

Öquist, G., and Huner, N.P. (2003). Photosynthesis of overwintering evergreen plants. Annu. Rev. Plant Biol. **54:** 329–355.

Oster, U., Tanaka, R., Tanaka, A., and Rüdiger, W. (2000). Cloning and functional expression of the gene encoding the key enzyme for chlorophyll *b* biosynthesis (CAO) from *Arabidopsis thaliana.* Plant J. **21:** 305–310.

Pogson, B., McDonald, K.A., Truong, M., Britton, G., and DellaPenna, D. (1996). *Arabidopsis* carotenoid mutants demonstrate that lutein is not essential for photosynthesis in higher plants. Plant Cell **8:** 1627–1639.

Roach, T., and Krieger-Liszkay, A. (2012). The role of the PsbS protein in the protection of photosystems I and II against high light in *Arabidopsis thaliana*. Biochim. Biophys. Acta **1817:** 2158–2165.

Ruban, A.V. (2016). Non-photochemical chlorophyll fluorescence quenching: mechanism and effectiveness in protection against photodamage. Plant Physiol. **170:** 1903–1916.

Schaller, S., Latowski, D., Jemioła-Rzemińska, M., Dawood, A., Wilhelm, C., Strzałka, K., and Goss, R. (2011). Regulation of LHCII aggregation by different thylakoid membrane lipids. Biochim. Biophys. Acta **1807:** 326–335.

Schneeberger, K., Ossowski, S., Lanz, C., Juul, T., Petersen, A.H., Nielsen, K.L., Jørgensen, J.E., Weigel, D., and Andersen, S.U. (2009). SHOREmap: simultaneous mapping and mutation identification by deep sequencing. Nat. Methods **6:** 550–551.

Sorek, N., Szemenyei, H., Sorek, H., Landers, A., Knight, H., Bauer, S., Wemmer, D.E., and Somerville, C.R. (2015). Identification of MEDIATOR16 as the *Arabidopsis* COBRA suppressor MONGOOSE1. Proc. Natl. Acad. Sci. USA **112:** 16048–16053.

Sylak-Glassman, E.J., Malnoë, A., De Re, E., Brooks, M.D., Fischer, A.L., Niyogi, K.K., and Fleming, G.R. (2014). Distinct roles of the photosystem II protein PsbS and zeaxanthin in the regulation of light harvesting in plants revealed by fluorescence lifetime snapshots. Proc. Natl. Acad. Sci. USA **111:** 17498–17503.

Takabayashi, A., Kurihara, K., Kuwano, M., Kasahara, Y., Tanaka, R., and Tanaka, A. (2011). The oligomeric states of the photosystems and the light-harvesting complexes in the Chl *b*-less mutant. Plant Cell Physiol. **52:** 2103–2114.

Tanaka, A., Ito, H., Tanaka, R., Tanaka, N.K., Yoshida, K., and Okada, K. (1998). Chlorophyll *a* oxygenase (CAO) is involved in chlorophyll *b* formation from chlorophyll *a.* Proc. Natl. Acad. Sci. USA **95:** 12719–12723.

Tardif, G., Kane, N.A., Adam, H., Labrie, L., Major, G., Gulick, P., Sarhan, F., and Laliberté, J.F. (2007). Interaction network of proteins associated with abiotic stress response and development in wheat. Plant Mol. Biol. **63:** 703–718.

Tomitani, A., Okada, K., Miyashita, H., Matthijs, H.C., Ohno, T., and Tanaka, A. (1999). Chlorophyll *b* and phycobilins in the common ancestor of cyanobacteria and chloroplasts. Nature **400:** 159–162.

Verhoeven, A.S., Adams, I.I.I., Demmig-Adams, B., Croce, R., and Bassi, R. (1999). Xanthophyll cycle pigment localization and dynamics during exposure to low temperatures and light stress in *vinca major.* Plant Physiol. **120:** 727–738.

Walters, R.G., and Horton, P. (1993). Theoretical assessment of alternative mechanisms for non-photochemical quenching of PS II fluorescence in barley leaves. Photosynth. Res. **36:** 119–139.

Weigel, D., and Glazebrook, J. (2006). Setting up *Arabidopsis* crosses. Cold Spring Harb. Protoc. **2006:** pdb.prot4623.

Woo, J.W., Kim, J., Kwon, S.I., Corvalán, C., Cho, S.W., Kim, H., Kim, S.-G., Kim, S.-T., Choe, S., and Kim, J.-S. (2015). DNA-free genome editing in plants with preassembled CRISPR-Cas9 ribonucleoproteins. Nat. Biotechnol. **33:** 1162–1164.